Supporting Information

3D Hierarchical Networks Constructed from Interlayer-Expanded MoS_2 Nanotubes and rGO as High-Rate and Ultra-Stable Anodes for Lithium/Sodium-Ion Batteries

Bingqing Ye[1], Zhou Cui[2], Zunxian Yang[*,1,3], Wenbo Wu[1], Yuliang Ye[1], Zihong Shen[1], Yuanqing Zhou[1], Qiaocan Huang[1], Songwei Ye[1], Zhiming Cheng[1],Hongyi Hong[1], Zongyi Meng[1], Zhiwei Zeng[1], Qianting Lan[1], Jiaxiang Wang[1], Ye Chen[1], Hui Zhang[1], Tailiang Guo[1,3], Yun Ye[1,3], Baisheng Sa[**,2,], Zhenzhen Weng[4], Yongyi Chen[4]

[1]National & Local United Engineering Laboratory of Flat Panel Display Technology, Fuzhou University, Fuzhou 350108, P. R. China.

[2]Multiscale Computational Materials Facility, and Key Laboratory of Eco-materials Advanced Technology, College of Materials Science and Engineering, Fuzhou University, Fuzhou 350100, P. R. China

[3]Mindu Innovation Laboratory, Fujian Science & Technology Innovation Laboratory For Optoelectronic Information of China, Fuzhou,350108, P.R. China

[4]Department of Physics, School of Physics and Information Engineering, Fuzhou University

* Corresponding author should be addressed. Tel.: +86 591 8789 3299; Fax: +86 591 8789 2643
E-mail: yangzunxian@hotmail.com (Z. Yang)
bssa@fzu.edu.cn (B Sa)

Number of pages: 22

Number of figures: 15

Number of tables: 3

Captions

Fig.S1 (a, b) Low-magnification and **(c)** High-magnification SEM image of MoS_2 nanotubes. **(d)** SEM image of MoS_2@GO-2 composite.

Fig.S2 FTIR spectra of the as-prepared MoS_2 nanotubes.

Fig.S3 High-magnification SEM images of NC-MoS_2@rGO-2 composite.

Fig.S4 TEM images of NC-MoS_2@rGO-2 composite.

Fig.S5 (a, b) Low-magnification images, **(c, d)** High-magnification SEM images, **(e-g)** TEM images, **(h)** HRTEM image, and **(i-m)** EDS mapping of NC-MoS_2 nanotubes.

Fig.S6 (a) Low-magnification and **(b, c)** High-magnification SEM images of NC-MoS_2@rGO-1 nanotubes. **(d)** Low-magnification and **(e, f)** High-magnification SEM images of NC-MoS_2@rGO-3 composite.

Fig.S7 XRD patterns of MoS_2 nanotubes and MoS_2@GO-2 composite.

Fig.S8 Discharge/charge voltage profiles of NC-MoS_2@rGO-2 electrode at different current densities for LIBs.

Fig.S9 Long-term cycling stability of NC-MoS_2@rGO-2 electrode at 1 A g^{-1} for LIBs.

Fig.S10 Cycling performance of NC-MoS_2, NC-MoS_2@rGO-1, NC-MoS_2@rGO-2

and NC-MoS_2@rGO-3 electrodes at 1 A g^{-1} for LIBs.

Fig.S11 Long-term cycling stability of NC-MoS_2@rGO-2 electrode at 10 A g^{-1} for LIBs.

Fig.S12 (a) Low-magnification and **(b)** High-magnification SEM images of NC-MoS_2@rGO-2 composite after 500 cycles at 2 A g^{-1}.

Fig.S13 (a) EIS and **(f)** the corresponding relationship plots between Z' and $\omega^{-1/2}$ of NC-MoS2@rGO-2 electrodes before cycles. **(c)** plots of Z' vs. $\omega^{-1/2}$ after different cycles at 0.2 A g^{-1} for LIBs.

Fig.S14 E versus t profile of NC-MoS_2@rGO-2 electrode for a single GITT during the lithiation process.

Fig.S15 (a) EIS and **(b)** Linear fits (relationship plot between Z' and $\omega^{-1/2}$) in the low-frequency region of NC-MoS_2@rGO-2 electrode before cycles for NIBs.

Table S1 Comparison of the cycling performance of NC-MoS_2@rGO-2 with the relevant anode materials for Li-ion batteries in the recently reported literature.

Table S2 Fitting parameters of NC-MoS_2@rGO-2 electrode for LIBs after different cycles.

Table S3 Comparison of the cycling performance of NC-MoS_2@rGO-2 with the recently reported MoS_2-based anode materials for Na-ion batteries in other literature.

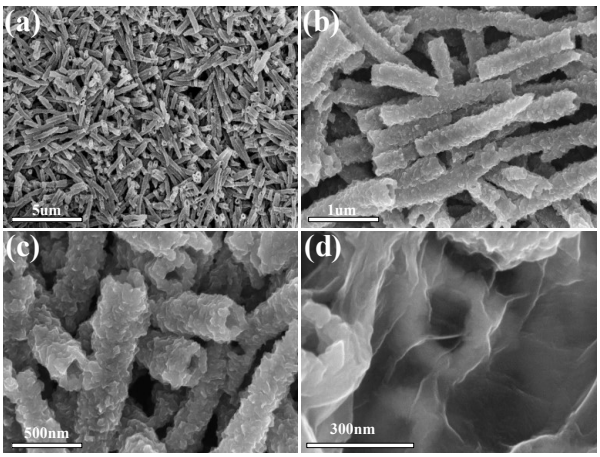

Fig.S1

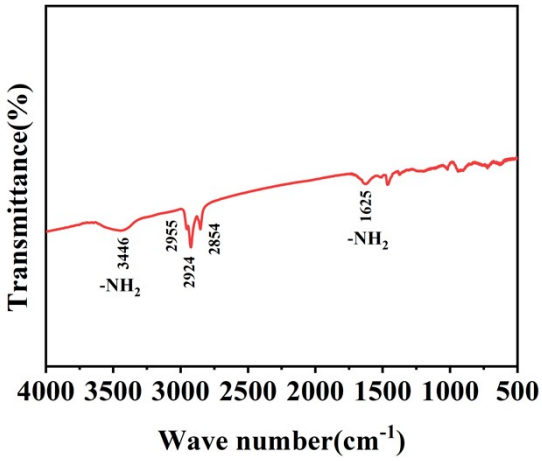
Transmittance(%)
3446
-NH2
2955
2924
2854
1625
-NH2
4000 3500 3000 2500 2000 1500 1000 500
Wave number(cm-1)

Fig.S2

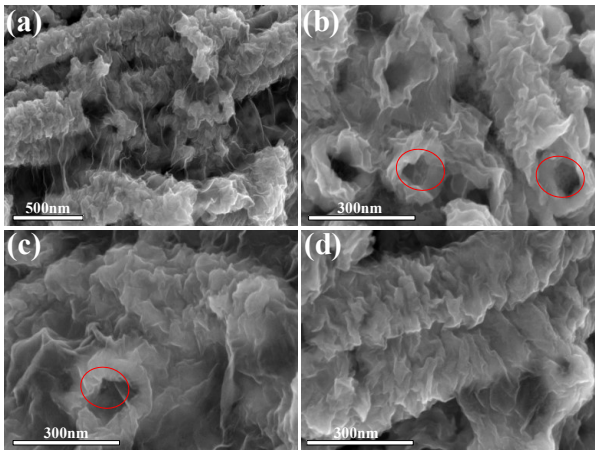

Fig.S3

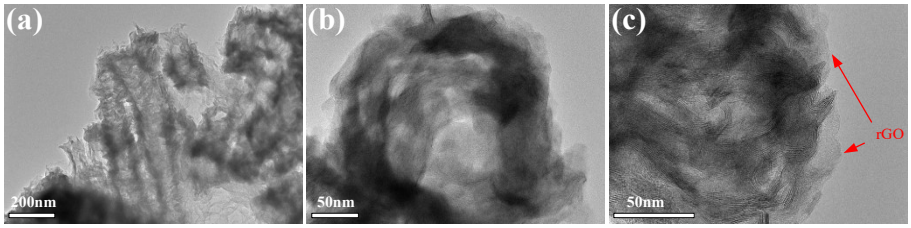

Fig.S4

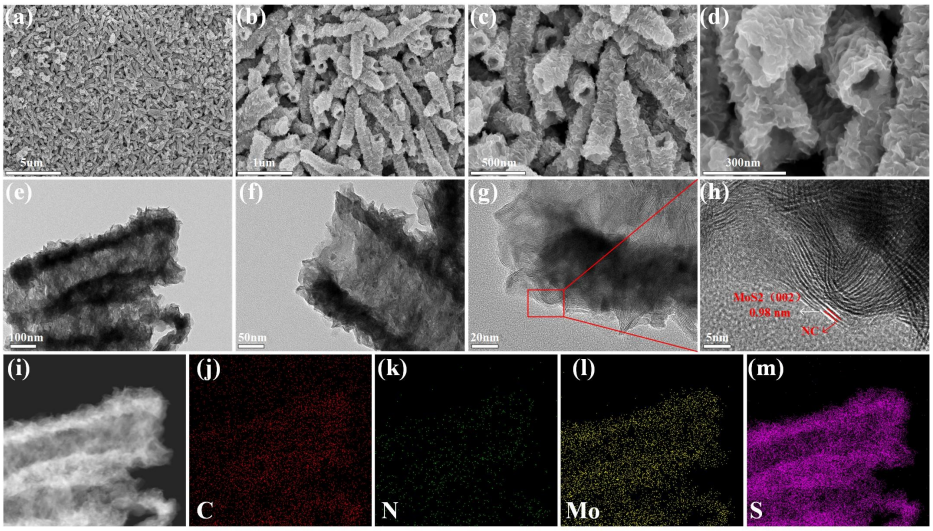
(a)
5μm
(b)
1μm
(c)
500nm
(d)
300nm
(e)
100nm
(f)
50nm
(g)
20nm
(h)
MoS2 (002)
0.98 nm
SC-2
5nm
(i)
(j)
C
(k)
N
(l)
Mo
(m)
S

Fig.S5

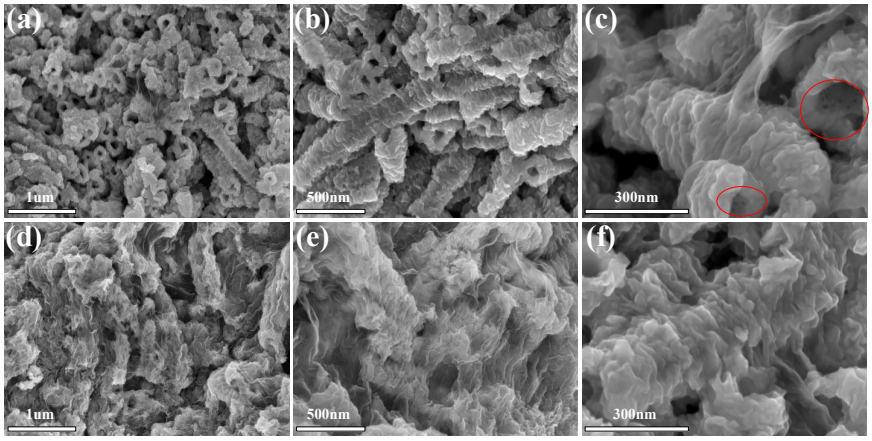

Fig.S6

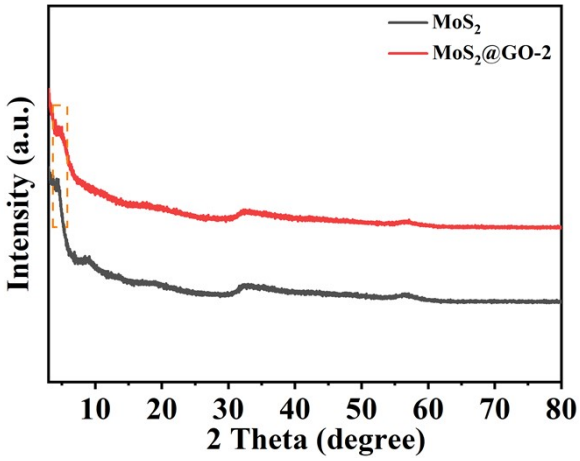
MoS2
MoS2@GO-2
Intensity (a.u.)
10
20
30
40
50
60
70
80
2 Theta (degree)

Fig.S7

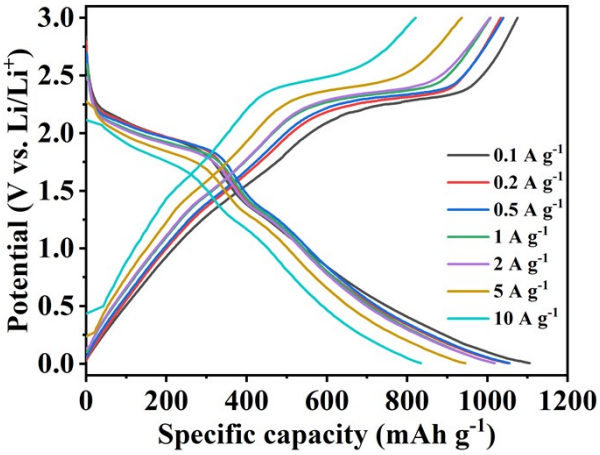
Potential (V vs. Li/Li+)
Specific capacity (mAh g-1)
0.1 A g-1
0.2 A g-1
0.5 A g-1
1 A g-1
2 A g-1
5 A g-1
10 A g-1

Fig.S8

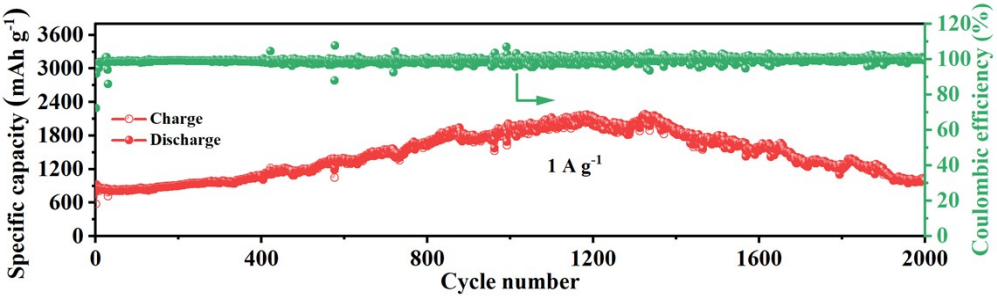
Specific capacity (mAh g-1)
Coulombic efficiency (%)
Cycle number
Charge
Discharge
1 A g-1
0
400
800
1200
1600
2000
600
1800
2400
3000
3600
20
40
60
80
100
120

Fig.S9

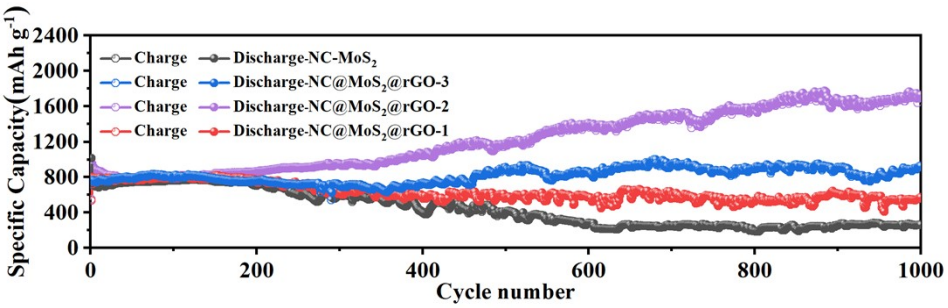
Specific Capacity(mAh g-1)
2400
2000
1600
1200
800
400
0
0
200
400
600
800
1000
Cycle number
Charge
Discharge-NC-MoS2
Charge
Discharge-NC@MoS2@rGO-3
Charge
Discharge-NC@MoS2@rGO-2
Charge
Discharge-NC@MoS2@rGO-1

Fig.S10

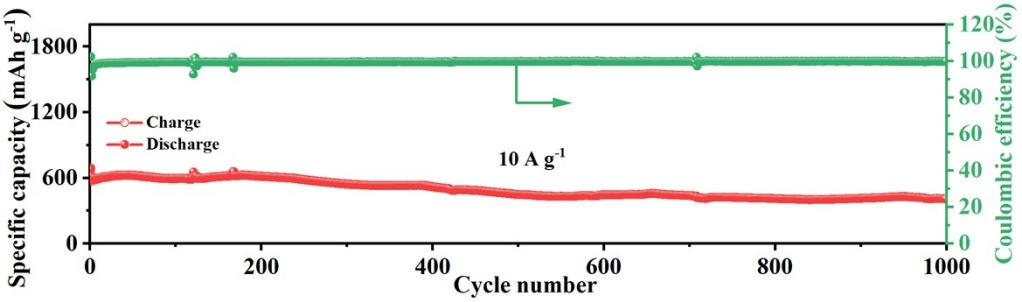
Specific capacity (mAh g-1)
1800
1200
600
0
Charge
Discharge
10 A g-1
0
200
400
600
800
1000
Cycle number
120
100
80
60
40
20
0
Coulombic efficiency (%)

Fig.S11

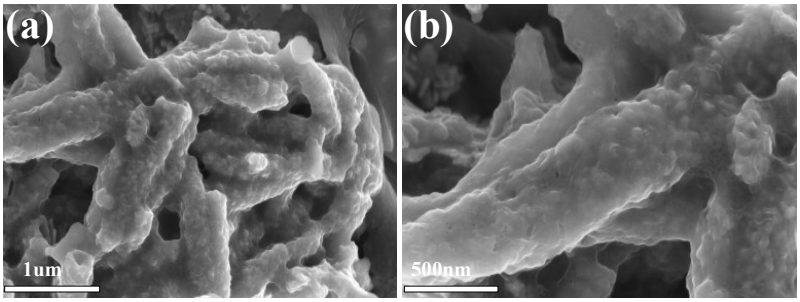

Fig.S12

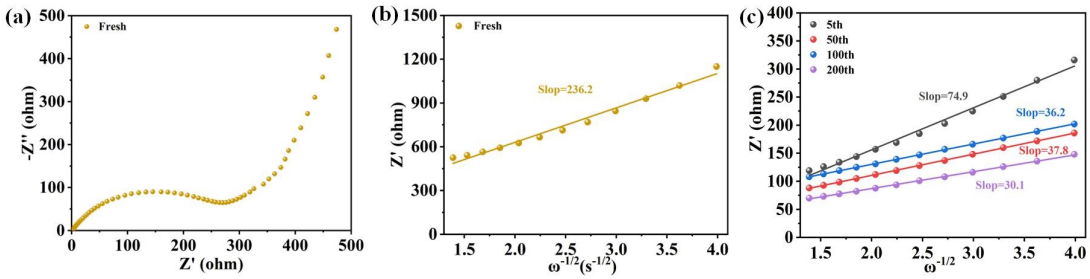
(a)
Fresh
-Z'' (ohm)
Z' (ohm)
(b)
Fresh
Slop=236.2
Z' (ohm)
ω^-1/2(s^-1/2)
(c)
5th
50th
100th
200th
Slop=74.9
Slop=36.2
Slop=37.8
Slop=30.1
Z' (ohm)
ω^-1/2

Fig.S13

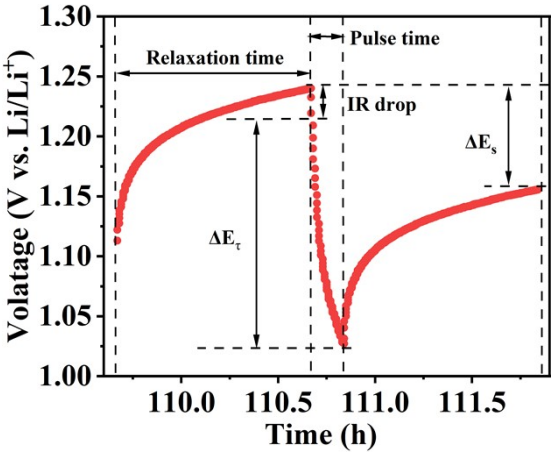
Relaxation time
Pulse time
IR drop
ΔE_s
ΔE_τ
Volatage (V vs. Li/Li+)
Time (h)
1.30
1.25
1.20
1.15
1.10
1.05
1.00
110.0
110.5
111.0
111.5

Fig.S14

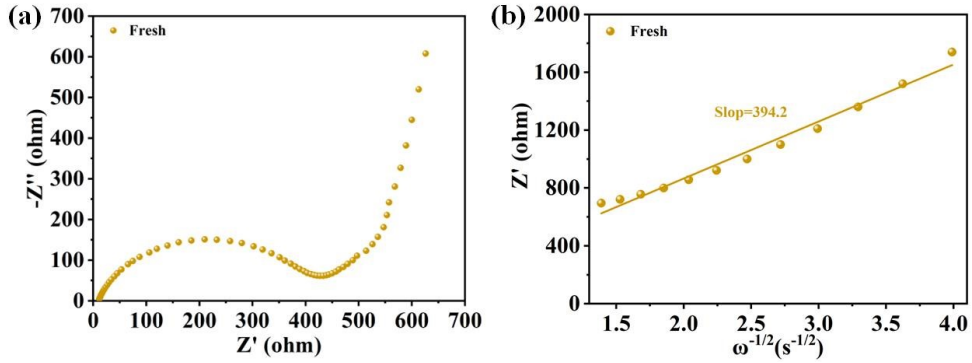
(a)
Fresh
-Z'' (ohm)
Z' (ohm)
0
100
200
300
400
500
600
700
(b)
Fresh
Slop=394.2
Z' (ohm)
ω^-1/2(s^-1/2)
0
400
800
1200
1600
2000
1.5
2.0
2.5
3.0
3.5
4.0

Fig.S15

Table S1

Materials	Current density (mAg^{-1})	(Cycles)	Capacity ($mAhg^{-1}$)	Reference
N-GRs/MoS_2	500 2000	200 600	925 547	[1]
WS_2/MoS_2@C/rGO hollow microspheres	500 1000	450 550	1036.5 701.8	[2]
3D NCMTs@A-MoS_2/RGO composite	1000	1000	544	[3]
MoS_2/C@G hybrid nanosheet	100 500	500 1000	691.7 662.7	[4]
MoS_2/graphene	100	150	813	[5]
MoS_2/m-C porous-hollow nanorods	200 1000 1250	100 100 350	1170 970 951	[6]
1T′-MoS_2/rhGO	200 5000	200 2000	1092 635	[7]
G-MoS_2 composite	5000	1500	539.9	[8]
CNT@NCT@W-MoS_2/C	500	200	734	[9]
MoS_2@rGO-CNTs	200 5000	200 1000	1226 745	[10]
M(S+C)/rGO	500 5000	200 200	1089 696	[11]
NC-MoS_2@rGO-2	200 200 1000 2000 5000 10000	200 500 2000 1500 6590 500	1308.6 1115.4 1034.3 774 528.4 407.9	This work

Table S2

Number of cycles	0	5	50	100	200
R_{ct} (Ω)	316.3	60.45	53.21	30.8	25.54
σ_w (Ω s^{-1})	236.2	74.9	37.8	36.2	30.1

Table S3

Materials	Current density (mAg^{-1})	(Cycles)	Capacity ($mAhg^{-1}$)	Reference
WS_2/MoS_2@C/rGO Hollow microspheres	100 500 1000	180 250 280	470.6 411.8 372.8	[2]
MoS_2@RGO	500	200	253.1	[12]
MoS_2@N-RGO	200 1000	200 300	328 250	[13]
MoS_2/m-C@a-C@Ti_3C_2	1000 2000	500 2000	331 212	[14]
MoS_2/m-C porous-hollow nanorods	200 500	300 500	397 350	[6]
SnS_2@MoS_2@rGO	100	100	396	[15]
G-MoS_2 composite	1000	200	256	[8]
CNT@NCT@W-MoS_2/C	1000 2000	100 100	335 283	[9]
rGO/MoS_2	1000	300	362.5	[16]
MoS_2@rGO composites	1000 2000	300 500	417.2 289.5	[17]
Ex-MoS_2/RGO@C	100	150	415	[18]
MoS_2-G microflower	200	100	500	[19]
MoS_2-C@C	500 2000	400 1000	463 312	[20]
NC-MoS_2@rGO-2	200 1000 2000	200 1000 1500	554.8 463.6 383.2	This work

References

[1] Z. P. Xiao, L. Z. Sheng, L. L. Jiang, Y. Y. Zhao, M. H. Jiang, X. Zhang, M. Y. Zhang, J. Y. Shi, Y. Q. Lin, Z. J. Fan, Nitrogen-doped graphene ribbons/MoS2 with ultrafast electron and ion transport for high-rate Li-ion batteries. **Chemical Engineering Journal**, **2021**, **408**: 127269.

[2] Y. Rao, J. Wang, P. H. Liang, H. J. Zheng, M. Wu, J. T. Chen, F. Shi, K. Yan, J. S. Liu, K. Bian, C. X. Zhang, K. J. Zhu, Heterostructured WS2/MoS2@carbon hollow microspheres anchored on graphene for high-performance Li/Na storage. **Chemical Engineering Journal**, **2022**, **443**: 136080.

[3] X. J. Liu, X. T. Zhang, S. H. Ma, S. S. Tong, X. J. Han, H. Wang, Flexible amorphous MoS2 nanoflakes/N-doped carbon microtubes/reduced graphite oxide composite paper as binder free anode for full cell lithium ion batteries. **Electrochimica Acta**, **2020**, **333**: 135568.

[4] B. Lan, X. Q. Zhang, Y. S. Wang, C. C. Wei, G. W. Wen, Constructing highly stable lithium storage materials by improving the bond strength of MoS2 to graphene via chitosan. **Carbon**, **2022**, **192**: 384-394.

[5] R. I. Pushparaj, D. Cakir, X. Zhang, S. Xu, M. Mann, X. D. Hou, Coal-Derived Graphene/MoS2 Heterostructure Electrodes for Li-Ion Batteries: Experiment and Simulation Study. **Acs Applied Materials & Interfaces**, **2021**, **13**(50): 59950-59961.

[6] L. Y. Jing, G. Lian, J. R. Wang, M. W. Zhao, X. Z. Liu, Q. L. Wang, D. L. Cui, C. P. Wong, Porous-hollow nanorods constructed from alternate intercalation of carbon

and MoS2 monolayers for lithium and sodium storage. **Nano Research**, **2019**, **12**(8): 1912-1920.

[7] Z. J. Mi, D. M. Hu, J. Y. Lin, H. Pan, Z. X. Chen, Y. Li, Q. L. Liu, S. M. Zhu, Anchoring nanoarchitectonics of 1T'-MoS2 nanoflakes on holey graphene sheets for lithium-ion batteries with outstanding high-rate performance. **Electrochimica Acta**, **2022**, **403**: 139711.

[8] Y. Li, S. Jiang, Y. Qian, X. D. Yan, J. Zhou, Z. Yi, N. Lin, Y. T. Qian, 2D interspace confined growth of ultrathin MoS2-intercalated graphite hetero-layers for high-rate Li/K storage. **Nano Research**, **2021**, **14**(4): 1061-1068.

[9] Y. H. Wang, Y. Yang, D. Y. Zhang, Y. B. Wang, X. K. Luo, X. M. Liu, J. K. Kim, Y. S. Luo, Inter-overlapped MoS2/C composites with large-interlayer-spacing for high-performance sodium-ion batteries. **Nanoscale Horizons**, **2020**, **5**(7): 1127-1135.

[10] J. Xia, R. X. Li, T. S. Wang, P. H. Yang, H. L. Zhou, J. J. Li, G. Y. Xiong, Y. L. Xing, S. C. Zhang, Structure-designed synthesis of 3D MoS2 anchored on ionic liquid modified rGO-CNTs inspired by a honeycomb for excellent lithium storage. **Journal of Materials Chemistry A**, **2020**, **8**(9): 4868-4876.

[11] S. Mathialagan,P. G. Priya, Mo2C-MoS2 embedded reduced graphene oxide nanohybrid: Epitaxial synthesis of Mo2C to augment the lithium storage properties of MoS2. **Carbon**, **2020**, **158**: 756-765.

[12] X. D. Zhang, K. L. Liu, S. J. Zhang, F. J. Miao, W. D. Xiao, Y. L. Shen, P. Zhang, Z. Wang, G. S. Shao, Enabling remarkable cycling performance of high-loading MoS2@Graphene anode for sodium ion batteries with tunable cut-off voltage.

Journal of Power Sources, **2020**, **458**: 228040.

[13] W. W. Zhan, M. Zhu, J. L. Lan, H. C. Yuan, H. J. Wang, X. P. Yang, G. Sui, All-in-One MoS2 Nanosheets Tailored by Porous Nitrogen-Doped Graphene for Fast and Highly Reversible Sodium Storage. **Acs Applied Materials & Interfaces**, **2020**, **12**(46): 51488-51498.

[14] J. W. Sun, S. L. Jiao, G. Lian, L. Y. Jing, D. L. Cui, Q. L. Wang, C. P. Wong, Hierarchical MoS2/m-C@a-C@Ti3C2 nanohybrids as superior electrodes for enhanced sodium storage and hydrogen evolution reaction. **Chemical Engineering Journal**, **2021**, **421**: 129680.

[15] X. L. Yu, C. M. Chen, R. X. Li, T. Yang, W. L. Wang, Y. Dai, Construction of SnS2@MoS2@rGO heterojunction anode and their half/ full sodium ion storage performances. **Journal of Alloys and Compounds**, **2022**, **896**: 162784.

[16] Yuxiang Luo, Xiaobo Ding, Xiangdong Ma, Dongdong Liu, Haikuo Fu, Xunhui Xiong, Constructing MoO2@MoS2 heterostructures anchored on graphene nanosheets as a high-performance anode for sodium ion batteries. **Electrochimica Acta**, **2021**, **388**: 138612.

[17] H. Chen, T. B. Song, L. B. Tang, X. M. Pu, Z. Li, Q. J. Xu, H. M. Liu, Y. G. Wang, Y. Y. Xia, In-situ growth of vertically aligned MoS2 nanowalls on reduced graphene oxide enables a large capacity and highly stable anode for sodium ion storage. **Journal of Power Sources**, **2020**, **445**: 227271.

[18] M. Feng, M. J. Zhang, H. Z. Zhang, X. H. Liu, H. B. Feng, Room-temperature carbon coating on MoS2/Graphene hybrids with carbon dioxide for enhanced sodium

storage. **Carbon**, **2019**, **153**: 217-224.

[19] S. Anwer, Y. X. Huang, B. S. Li, B. Govindan, K. Liao, W. J. Cantwell, F. Wu, R. J. Chen, L. X. Zheng, Nature-Inspired, Graphene-Wrapped 3D MoS2 Ultrathin Microflower Architecture as a High-Performance Anode Material for Sodium-Ion Batteries. **Acs Applied Materials & Interfaces**, **2019**, **11**(25): 22323-22331.

[20] Z. Y. Li, S. Y. Liu, B. P. Vinayan, Z. Zhao-Karger, T. Diemant, K. Wang, R. J. Behm, C. Kubel, R. Klingeler, M. Fichtner, Hetero-layered MoS2/C composites enabling ultrafast and durable Na storage. **Energy Storage Materials**, **2019**, **21**: 115-123.